Title

Mortalin/HSPA9 targeting selectively induces KRAS tumor cell death by perturbing mitochondrial membrane permeability.

Journal

Oncogene, 39(21)

Authors

Wu, Pui-Kei
Hong, Seung-Keun
Starenki, Dmytro
et al.

Publication Date

2020-05-01

DOI

10.1038/s41388-020-1285-5

Peer reviewed

HHS Public Access

Author manuscript

Oncogene. Author manuscript; available in PMC 2020 October 14.

Published in final edited form as:

Oncogene. 2020 May ; 39(21): 4257–4270. doi:10.1038/s41388-020-1285-5.

Mortalin/HSPA9 targeting selectively induces *KRAS* tumor cell death by perturbing mitochondrial membrane permeability

Pui-Kei Wu[1], **Seung-Keun Hong**[1], **Dmytro Starenki**[1], **Kiyoko Oshima**[2], **Hao Shao**[3], **Jason E. Gestwicki**[3], **Susan Tsai**[4], **Jong-In Park**[1,#]

[1]Department of Biochemistry, Medical College of Wisconsin, Milwaukee, WI 53226, USA

[2]Department of Pathology, Johns Hopkins University, School of Medicine, Baltimore, MD 21287, USA

[3]Department of Pharmaceutical Chemistry, University of California San Francisco, San Francisco, CA 94158, USA

[4]LaBahn Pancreatic Cancer Program and Department of Surgery, Medical College of Wisconsin, Milwaukee, WI 53226, USA

Abstract

The mitochondrial HSP70 chaperone mortalin (HSPA9/GRP75) is often upregulated and mislocalized in MEK/ERK-deregulated tumors. Here, we show that mortalin depletion can selectively induce death of immortalized normal fibroblasts IMR90E1A when combined with K-Ras^{G12V} expression, but not with wild type K-Ras expression, and that K-Ras^{G12V}-driven MEK/ERK activity is necessary for this lethality. This cell death was attenuated by knockdown or inhibition of adenine nucleotide translocase (ANT), cyclophilin D (CypD), or mitochondrial Ca^{2+} uniporter (MCU), which implicates a mitochondria-originated death mechanism. Indeed, mortalin depletion increased mitochondrial membrane permeability and induced cell death in *KRAS*-mutated human pancreatic ductal adenocarcinoma (PDAC) and colon cancer lines, which were attenuated by knockdown or inhibition of ANT, CypD, or MCU, and occurred independently of TP53 and p21^{CIP1}. Intriguingly, JG-98, an advanced MKT-077 derivative, phenocopied the lethal effects of mortalin depletion in K-Ras^{G12V}-expressing IMR90E1A and *KRAS*-mutated tumor cell lines in vitro. Moreover, JG-231, a JG-98 analog with improved microsomal stability effectively suppressed the xenograft of MIA PaCa-2, a K-Ras^{G12C}-expressing human PDAC line, in athymic

[#]**Corresponding author at:** Department of Biochemistry, Medical College of Wisconsin, 8701 Watertown Plank Road, Milwaukee, WI 53226, USA, Phone: +1 (414) 955-4098, Fax: +1 (414) 955-6510, jipark@mcw.edu (J.-I. Park).

Author contributions

Conceptualization, P.W. and J.P.; Methodology, P.W., S.H., D.S., and J.P; Investigation, P.W., S.H., D.S., and J.P.; Formal Analysis, P.W., S.H., D.S., K.O., and J.P.; Writing – Original Draft, P.W. and J.P.; Writing – Review & Editing, P.W., J.G., S.T., and J.P.; Funding Acquisition, J.P.; Resources, S.T., H.S. and J.G.; Supervision, J.P.

Competing interests

J.G is an inventor on a US patent application that includes HSP70 modulators. Other authors declare that they have no competing interests.

Data and materials availability

All data needed to evaluate the conclusions in the paper are present in the paper or the Supplementary Materials. JG series HSP70 modulators are available from J.G. under a material transfer agreement with UCSF.

nude mice. These data demonstrate that oncogenic *KRAS* activity sensitizes cells to the effects of mortalin depletion, suggesting that mortalin has potential as a selective therapeutic target for *KRAS*-mutated tumors.

Keywords

KRAS; MEK/ERK; mortalin; mitochondrial permeability; cell death

INTRODUCTION

A mutation in *KRAS* is one of the most frequently detected oncogenic alterations and is a key therapeutic target. Indeed, recent success in developing small molecule inhibitors that directly target K-Ras^{G12C} heralds advances in precision treatments of *KRAS* tumors[6, 40]. Yet direct Ras targeting is still at an early stage, and growing evidence indicates the ability of tumor cells to develop therapeutic resistance despite their initial responsiveness to a precision cancer drug targeting of downstream pathways of Ras[24, 27, 28, 44, 51]. Therefore, additional therapeutic strategies are required to effectively treat *KRAS* tumors and targeting of a molecular process selectively required for the tumors is a promising strategy.

Mitochondria serve a key role for tumor cell proliferation and survival thorough their pivotal roles in metabolism, including energy and building block generation. Paradoxically, mitochondria can also cause tumor cell death through their central role in cell death, which is often triggered upon permeabilization of their membrane[30, 31]. For example, permeabilized outer mitochondrial membrane can release various death factors from the intermembrane space whereas a mitochondrial membrane-spanning permeability transition pore (MPTP) can cause metabolic catastrophe[8, 30], although the exact molecular composition and mechanisms of MPTP requires better understanding[3, 17, 22, 39]. Of note, cell death originating from mitochondria is often mediated by various mitochondrial channels and regulators, including adenine nucleotide translocase (ANT), mitochondrial Ca^{2+} uniporter (MCU), and cyclophilin D (CypD), and can be caused by various metabolic stresses, including deregulated mitochondrial redox or Ca^{2+} flux[30, 31]. Because the necessity of metabolic reprogramming for oncogenic transformation would inevitably increase the chance for mitochondrial stress[12, 31], it is conceivable that tumor cells have developed a protective mechanism (or mechanisms) in this context and a vulnerability in this mechanism, if identified, may be exploited for therapy.

Mortalin (HSPA9/GRP75/PBP74) is a member of heat shock protein 70 (HSP70) family localized in mitochondria[11, 32]. Mortalin is often upregulated and mislocalized in tumor cells and can facilitate tumor cell proliferation/survival, stemness, epithelial-mesenchymal transition, and angiogenesis[7, 25, 37, 43, 57, 64]. We previously demonstrated that mortalin facilitates tumor cell proliferation and survival by modulating MEK/ERK activity[23, 59, 60] and mitochondrial bioenergetics[48]. Moreover, we recently reported that deregulated MEK/ERK activity in *BRAF*-mutated tumor cells increase mitochondrial permeability whereas mortalin counteracts this increase by limiting the physical interaction between ANT3 and CypD and, hence, mortalin depletion in these cells results in perturbed

mitochondrial permeability, which causes robust tumor cell death[61]. Based upon these findings, we hypothesized that mortalin is a candidate target exploitable to selectively induce mitochondrial cell death in MEK/ERK-dependent tumors and predicted that mortalin targeting would selectively suppress *KRAS*-mutated tumors because these tumors often exhibit deregulated MEK/ERK activity.

In this study, we tested this possibility by determining (i) whether mortalin depletion induces lethality conditional upon the presence of K-Ras^{G12V}, but not wild type K-Ras, in immortalized normal human diploid fibroblasts IMR90E1A; (ii) whether this cell death requires K-Ras^{G12V}-driven MEK/ERK activity and the mitochondrial channels/regulators ANT, CypD, and MCU; and (iii) whether mortalin depletion suppresses *KRAS*-mutated tumor cells by perturbing mitochondrial permeability. Moreover, we determined whether chemical inhibition of mortalin can phenocopy mortalin depletion in K-Ras^{G12V}-expressing IMR90E1A cells and effectively suppresses a *KRAS*-mutated pancreatic ductal adenocarcinoma (PDAC) cell line xenograft in mice. Collectively, our data support the potential of mortalin as a therapeutic target selective for *KRAS* mutant tumor cells.

RESULTS

Mortalin depletion induces selective lethality in IMR90E1A cells expressing K-Ras^{G12V}, but not wild type K-Ras:

To determine the significance of mortalin in cells expressing an oncogenic K-Ras mutant (K-Ras^{mut}), we examined the effects of concurrent mortalin depletion and expression of K-Ras^{G12V}, or of wild type K-Ras (K-Ras^{WT}), in IMR90E1A cells. As determined by Western blotting and trypan blue exclusion assays, mortalin knockdown robustly induced lethality in IMR90E1A cells expressing K-Ras^{G12V}, but not K-Ras^{WT}, although neither mortalin knockdown nor K-Ras^{G12V} expression was lethal to IMR90E1A cells when used singly (Fig. 1A and 1B). Consistent with this, mortalin knockdown substantially increased lamin A cleavage, an apoptosis marker[41], specifically in cells expressing K-Ras^{G12V}, but not K-Ras^{WT}, although its effects on poly-(ADP-ribose)-polymerase (PARP) cleavage was very mild (Fig. 1A). Indeed, mortalin knockdown increased apoptosis in cells expressing K-Ras^{G12V}, but not K-Ras^{WT}, as determined by scoring cells co-stained for annexin V/propidium iodide (Fig. 1C; Fig. S1A) and cells arrested in sub-G0/G1 phase (Fig. 1D; Fig. S1B). Moreover, mortalin depletion augmented K-Ras^{G12V}-induced p21^{CIP1} expression in these cells although it did not affect p16^{INK4a} levels (Fig. 1A). Under these conditions, pretreatment with selumetinib (AZD6244, MEK1/2 inhibitor) or SCH772984 (ERK1/2 inhibitor) substantially attenuated cell death (Fig. 1E), lamin A cleavage and p21^{CIP1} expression (Fig. 1F and 1G). These data demonstrate that mortalin depletion can selectively induce lethality in K-Ras^{G12V}-expressing IMR90E1A cells, for which MEK/ERK activity is necessary.

ANT3, CypD, and MCU are required for the lethality caused by concurrent K-Ras^{G12V} expression and mortalin depletion:

ANT can interact with CypD, the gatekeeper of MPTP[9], and this interaction has been implicated in mitochondrial membrane permeabilization, which is often triggered by

increased Ca^{2+} flux through MCU[30, 31]. We determined whether knockdown or inhibition of these proteins can rescue IMR90E1A cells from the lethal effects of concurrent K-Ras^{G12V} expression and mortalin depletion.

Knockdown of ANT3, using two different shRNA constructs, substantially attenuated mortalin depletion-induced cell death and lamin A cleavage in K-Ras^{G12V}-expressing IMR90E1A cells (Fig. 2A and 2B). Similarly, knockdown of CypD and MCU also rescued these cells from mortalin knockdown (Fig. 2C to 2F). In contrast, knockdown of ANT3, CypD, or MCU did not markedly affect mortalin depletion-induced p21^{CIP1} expression in these cells (Fig. 2B and 2D), suggesting that mortalin regulates p21^{CIP1} via a mechanism independent of these mitochondrial proteins. Consistent with knockdown of ANT3, CypD, or MCU, cyclosporin A, which inhibits the isomerase activity of CypD and displaces it from MPTP[13], and nelfinavir, which inhibits ANT[58] and mitochondrial Ca^{2+} influx[50], rescued K-Ras^{G12V}-expressing IMR90E1A cells from mortalin knockdown (Fig. 2G). These data suggest that the regulators of mitochondrial membrane permeability mediate cell death caused by concurrent K-Ras^{G12V} expression and mortalin depletion.

Mortalin is upregulated in PDAC and is required for survival and proliferation of K-Ras^{mut} PDAC cells:

Observing the specific relationship between mortalin and K-Ras^{G12V}, we sought to determine the significance of mortalin in K-Ras^{mut} tumors. Given the high frequency of *KRAS* mutation (>95%) and its etiological significance in PDAC[5], we conducted immunohistochemistry of 51 cases of human PDAC tissues to find a strong correlation between mortalin protein levels and tumor malignancy (Fig. 3A and 3B). Consistent with this, the human K-Ras^{mut} PDAC cell lines, AsPC-1 (K-Ras^{G12D}), MIA PaCa-2 (K-Ras^{G12C}), and PANC-1 (K-Ras^{G12D}) expressed mortalin much higher than primary normal human fibroblasts and as highly as MCF7 breast cancer cell line (Fig. 3C). MCF7 cells were shown to express higher levels of mortalin relative to different tumor lines derived from human tumors of breast, prostate, colon, lung, and brain[57]. In correlation with mortalin levels, these PDAC cells exhibited upregulated levels of HSP60, a key partner of mortalin in different biological processes, including tumor cell proliferation and survival[56]. However, in contrast, these PDAC cell lines did not exhibit notable upregulation of other HSP70 family paralogs, HSC70, HSP72, and BiP/GRP78 (Fig. 3C). These PDAC cell lines also exhibited markedly downregulated p21^{CIP1} and p16^{INK4a} expression (Fig. 3C).

We next determined the effects of mortalin depletion in AsPC-1, MIA PaCa-2, and PANC-1 cells. Infection of these PDAC cells with lentiviruses expressing two different shRNA targeted to mortalin mRNA consistently suppressed cell viability (Fig. 3D). Along with these effects, mortalin knockdown increased, at varied degrees, lamin A cleavage and p21^{CIP1} levels in cells, while not affecting PARP and p16^{INK4A} levels (Fig. 3E). Because these surrogate makers were not highly consistent in these cells, we also determined HMGB1 release, a necrosis marker also associated with MPTP-induced cell death[2]. Indeed, HMGB1 was detected in the cell culture media conditioned by these PDAC cells (Fig. 3E). These data suggest that mortalin is required for proliferation and survival of K-Ras^{mut} PDAC cells.

Mortalin depletion induces cell death by increasing mitochondrial permeability in K-Ras^{mut} tumor cells:

We determined whether altered mitochondrial permeability underlies mortalin depletion-induced lethality in K-Ras^{mut} tumor cells. Consistent with the effects observed in K-Ras^{G12V}-expressing IMR90E1A cells, knockdown of ANT3 and MCU substantially inhibited cell death and lamin A cleavage induced by mortalin depletion in MIA PaCa-2 cells (Fig. 4A and 4B). The CypD inhibitor cyclosporin A, the ANT inhibitor nelfinavir, and the MCU inhibitors ruthenium red[4] and KB-R7943[45] also rescued MIA PaCa-2 cells from mortalin knockdown, as determined by trypan blue exclusion assay (Fig. 4C) and annexin V/PI staining (Fig. 4D; Fig. S2). We next determined the effects of mortalin depletion on mitochondrial permeability by conducting the calcein-acetyoxymethyl release assay[52], also known as “calcein labelling”. Indeed, mortalin depletion abolished mitochondrial calcein retention in MIA PaCa-2 cells, while knockdown of ANT3 or MCU effectively attenuated these effects of mortalin depletion (Fig. 4E; Fig. S3A). Moreover, cells pretreated with cyclosporin A, nelfinavir, ruthenium red, and KB-R7943 exhibited enhanced ability to retain mitochondrial calcein in the face of mortalin depletion (Fig. 4F; Fig. S3B). These data suggest that the lethality induced by mortalin depletion in K-Ras^{mut} tumor cells is attributed to perturbed mitochondrial permeability.

TP53 and p21^{CIP1} are not necessary for mortalin depletion to induce cell death via altered mitochondrial permeability in K-Ras^{mut} tumor cells:

It has been previously shown that TP53 can facilitate mitochondrial permeabilization through its interaction with CypD[52]. Because all the PDAC cell lines tested in our study harbor a mutation in *TP53* (AsPC-1, TP53^{C135fs*35}; MIA PaCa-2, TP53^{R248W}; and PANC-1, TP53^{R273H}), we determined whether TP53 is dispensable for the lethality caused by mortalin depletion in K-Ras^{mut} tumor cells using an isogenic somatic knockout series of HCT116 (K-Ras^{G13D}, TP53^{wt}, p21^{wt}) colorectal carcinoma line. Using this knockout series, we also determined the significance of p21^{CIP1} because it is a key TP53 effector and because mortalin knockdown induced p21^{CIP1} in K-Ras^{mut}-expressing cells.

Mortalin knockdown induced cell death in HCT116 cells as well as in their progenies deficient of TP53 (TP53$^{-/-}$) or p21^{CIP1} (p21$^{-/-}$) although the parental cells exhibited slightly higher death rates than TP53$^{-/-}$ cells but slightly lower rates than p21$^{-/-}$ cells did, as determined by trypan blue exclusion assays (Fig. 5A to 5C) and Western blotting of lamin A cleavage (Fig. 5D). In all these cells, the ANT inhibitor bongkrekic acid[15], cyclosporin A, and nelfinavir attenuated mortalin depletion-induced death in a dose-dependent manner (Fig. 5A to 5C). These data demonstrate that TP53 and p21^{CIP1} are not necessary for mortalin depletion to trigger mitochondrial death in K-Ras^{mut} tumor cells.

Advanced MKT-077 derivatives phenocopy mortalin depletion and effectively suppress K-Ras^{mut} tumor cells:

MKT-077, a water soluble benzothiazole-rhodacyanine[29], binds to a well conserved negatively charged pocket close to the nucleotide binding site of human HSP70 paralogs[42]. Being a mitochondrial membrane potential ($\Delta\psi_m$)-sensitive delocalized lipophilic cation, MKT-077 mainly partitions into mitochondria[36], and its interaction with mortalin in vivo

was demonstrated by affinity purification, although it also interacted with HSC70 (HSPA8) and F-actin[34, 55]. Given these characteristics of MKT-077, we sought to use MKT-077 and its advanced derivatives for a "proof-of-concept demonstration" of mortalin targeting in K-Ras^{mut} tumors.

Indeed, MKT-077 exhibited much lower IC_{50} values than its $\Delta\psi_m$-insensitive neutral derivative, YM-08[35], in MIA-PaCa-2, AsPC-1, and PANC-1 cells (Fig. 6A). Observing these effects, we determined the sensitivity of these cells to JG-98, an MKT-077 derivative with improved affinity and selectivity for the HSP70 binding pocket[46]. Our IC_{50} analysis revealed that JG-98 has higher potency than MKT-077 and JG-258, a functional moiety-lacking control compound for JG-98[46] in MIA PaCa-2, AsPC-1, and HCT116 cells (Fig. 6B). Remarkably, very similar to the effects of mortalin depletion, JG-98 selectively induced lethality in IMR90E1A cells upon expression of K-Ras^{G12V}, but not K-Ras^{WT} (Fig. 6C). However, MKT-077 or JG-258 did not exhibit similar potency, as determined at the same or much higher dose ranges (Fig. 6C).

We next evaluated *in vivo* efficacy of JG-231, an analog of JG-98 with improved pharmacokinetics and bioavailability[46], in MIA PaCa-2 xenografts in athymic nude mice. When administered intraperitoneally, JG-231 effectively suppressed growth of the tumor xenografts (Fig. 7A to C) without causing significant loss of animal body weight (Fig. 7D). JG-231 treatment also increased lamin A cleavage and p21^{CIP1} expression in the tumors harvested at the end of the treatment (Fig. 7E). Along with these effects, JG-231-treated tumors exhibited substantially decreased cytochrome *c* oxidase levels with the exception of one tumor (Fig. 7E), suggesting that JG-231 incurred mitochondria damages. Moreover, JG-231 treatment increased MEK1/2 phosphorylation in tumors (Fig. 7E), which is consistent with its effects in *BRAF*-mutant tumor xenografts in mice[61]. These data strongly support the feasibility of exploiting mortalin to selectively suppress K-Ras^{mut} tumors.

DISCUSSION

Our data demonstrate that, when combined with K-Ras^{mut} expression, mortalin depletion can trigger robust cell death associated with altered mitochondrial membrane permeability. Our data suggest that this conditional lethality is driven by K-Ras^{mut}–induced MEK/ERK activity and is mediated by ANT and CypD. These findings are consistent with our recent observation that B-Raf^{V600E} tumor cells undergo ANT/CypD-mediated cell death in the absence of mortalin in a MEK/ERK-dependent manner[61]. Therefore, mortalin appears to have potential as a therapeutic target selective to not only B-Raf^{mut}– but also K-Ras^{mut}–driven tumors, wherein deregulated MEK/ERK activity is the common denominator. These findings strongly support our hypothesis that mortalin is a guardian of MEK/ERK-deregulated tumor cells against the lethal risk associated with mitochondrial permeability regulation, and we predict that this risk is inherent and exploitable in any MEK/ERK- and mortalin-dependent tumors. Exploitation of mitochondrial death machinery has been considered as a promising strategy for cancer therapy[30, 31], and it may also be relevant for the treatment of *KRAS* tumors, especially PDAC, given multiple evidences supporting mitochondria dependency of these tumor types[21, 38, 63]. Our current and previous studies consistently suggest mortalin as a candidate target for implementing this strategy.

Molecular chaperones can facilitate tumorigenesis by altering the stability or activity of client proteins involved in diverse cellular processes[26]. We recently identified ANT3 as a novel client for mortalin and demonstrated that a highly coordinated regulation of ANT3 by mortalin and MEK/ERK is critical for the survival of *BRAF* mutant tumors[61]. The present study extends this finding to *KRAS* tumor cells and provides consistent evidence that mortalin has pivotal role in suppressing the lethal potential of ANT3 in MEK/ERK-dependent tumors. ANT proteins play essential roles in cellular bioenergetics by mediating ATP/ADP exchange across the mitochondrial inner membrane[8]. If these processes are impaired, ANT can promote cell death by complexing with CypD[14, 15], although molecular mechanisms underlying this death machinery is yet unclear and a subject of intensive investigation. Because successful reprogramming of bioenergetics is critical for *KRAS* and *BRAF* tumorigenesis[16, 53], the sensitivity of *KRAS* and *BRAF* tumor cells to mortalin depletion may be attributed to a failure of ANT function in the context of MEK/ERK-driven bioenergetic reprogramming. Nevertheless, additional mechanistic scenarios may also be available. For example, a recent study suggested that ANT can induce mitochondrial cell death via a mechanism independent of its ability to exchange ATP/ADP[20]. This possibility remains to be tested in our future study.

Our finding of mortalin upregulation in PDAC tissues is consistent with recent reports of mortalin upregulation in PDAC as well as in other tumors exhibiting aberrant MEK/ERK activity, i.e., non-small cell lung carcinoma and ovarian carcinoma[10, 49, 62]. Importantly, mortalin in these tumors has been proposed as a prognostic marker for poor patient survival[10, 49, 62], and the data in the present study may provide insights into the molecular mechanisms by which mortalin facilitates the development of these tumors. Intriguingly, while TP53 mutations are detected in more than 50% of PDAC cases[1], mortalin depletion effectively suppressed all three TP53-mutated PDAC cell lines in our study. Moreover, the data from TP53-deficient ($TP53^{-/-}$) HCT116 progeny cells confirm the dispensability of TP53 for mortalin depletion-induced lethality in *KRAS* tumor cells. As such, we conclude that mortalin depletion triggers mitochondrial death independent of TP53. This is intriguing because tumor suppressive effects of mortalin depletion/inhibition have been partly attributed to its ability to sequester TP53[33, 54], and because TP53 is known to trigger mitochondrial permeabilization and subsequent cell death by directly interacting with CypD[52]. Of note, we showed that mortalin directly interacts with ANT but not with CypD while it inhibits the interaction between ANT3 and CypD[61]. Taken together, it is conceivable that mortalin and TP53 may comprise two independent regulators of mitochondrial permeabilization, which work in an opposing context.

In summary, our findings suggest that mortalin facilitates survival and proliferation of *KRAS* tumor cell by preventing MEK/ERK-driven mitochondrial permeabilization and that mortalin has potential as a therapeutic target for *KRAS* tumors irrespective of TP53 status. Importantly, although most *KRAS* tumors are MEK/ERK-dependent, therapeutic effects of MEK/ERK inhibition are not satisfactory due to the ability of tumor cells to develop therapy resistance[27, 44]. Development of diverse therapeutic strategies is therefore necessary and mortalin dependency of *KRAS* tumor cells demonstrated in this study may provide an idea for the development of strategy.

MATERIALS AND METHODS

Cell lines and reagents

IMR90E1A, a gift from Dr. Yuri Lazebnik (CSHL), were maintained in Dulbecco's minimal essential medium (DMEM, Invitrogen, Carlsbad, CA, USA) supplemented with 10% fetal bovine serum (FBS), 1% sodium pyruvate, and 1% nonessential amino acids. MiaPaCa-2 (ATCC) and PANC-1 (ATCC) were cultured in Dulbecco's minimal essential medium (Invitrogen) supplemented with 10% fetal bovine serum, 100 U/ml of penicillin, and 100 μg/ml of streptomycin. AsPC-1 (ATCC) was maintained in RPMI 1640 medium (Invitrogen) supplemented with 10% fetal bovine serum, 100 U/ml of penicillin, and 100 μg/ml of streptomycin. HCT116 and its $TP53^{-/-}$ and $p21^{-/-}$ progenies were obtained from Dr. Bert Vogelstein (Johns Hopkins Univ.) and were grown in McCoy's 5A medium (Invitrogen) supplemented with 10% FBS. Cell lines within 10 passages after acquisition were used for experiments in this study. All cell lines were authenticated prior to use by short tandem repeat DNA profiling and were negative for mycoplasma contamination.

Cyclosporine A, nelfinavir mesylate hydrate, and MKT-007 were purchased from Sigma-Aldrich (St. Louis, MO). AZD6244, SCH772984, and KB-R7943 were purchased from Selleck Chemicals (Houston, TX), ChemieTek (Indianapolis, IN), and Abcam (Cambridge, MA), respectively. Bongkrekic acid and ruthenium red were purchased from Santa Cruz Biotechnology (Santa Cruz, CA). JG-98, JG-258 and JG-231 were synthesized as previously reported[46].

Plasmids, RNA interference, and recombinant viruses

The lentiviral K-Ras^{G12V} expression system, pHAGE-K-Ras^{G12V}, was generated by ligating a human K-Ras^{G12V}–encoding gene (a gift from Dr. Bob Deschenes, Univ. South Florida) into NotI/XhoI sites of pHAGE-GFP. pHAGE-K-Ras^{WT} was generated by site-directed mutagenesis of pHAGE-K-Ras^{G12V} using TGTGGTAGTTGGAGCTGGTGGCGTAGGCAAGAGTG and CACTCTTGCCTACGCCACCAGCTCCAACTACCACA. Construction of the lentiviral small hairpin RNA expression systems targeting human mortalin, pLL3.7-shMort#1 and pLL3.7-shMort#2, were previously described[59]. pLKO.1-shANT3 (TRCN0000045014 and TRCN0000045015), pLKO.1-shCypD (TRCN0000232681 and TRCN0000232682), and pLKO.1-shMCU (TRCN0000133861 and TRCN0000416434) constructs were purchased from Sigma-Aldrich. Lentivirus was generated and used as previously described[18].

Immunoblotting

For immunoblotting, equal amount of proteins in cell lysates in 62.5 mM Tris (pH 6.8)/2% SDS containing the protease and phosphatase inhibitor cocktails were resolved by SDS-PAGE, transferred to polyvinylidene difluoride membranes (Bio-Rad, Hercules, CA, USA), and blocked with 5% nonfat dry milk or BSA in 0.1 M Tris (pH 7.5)/0.9% NaCl/0.05% Tween 20 prior to blotting. Antibodies and their dilutions are as follows: Ras (#3339), 1 : 2500; phospho-MEK1/2 (Ser217/221 for MEK1 and Ser222/226 for MEK2, #9121), 1 : 2500; MEK1/2 (#9122), 1 : 2500; ERK1/2 (#9102), 1 : 2500; cleaved lamin A (#2035), 1 : 2500; PARP (#9542), 1 : 2500; BiP (#3183), 1 : 5000, MCU (#14977), 1 : 2500; CoxIV

(#4850), 1 : 2500 (Cell Signaling Technology, Boston, MA, USA); phospho-ERK1/2 (Thr202/Tyr204, sc-16982), 1 : 2500 ; mortalin (sc-133137), 1 : 5000; $p21^{CIP1}$ (sc-56335), 1 : 2500; TP53 (sc-126), 1 : 2500; CypD (sc-376061), 1 : 2500 (Santa Cruz Biotechnology, Santa Cruz, CA, USA); β-actin (A2228), 1 : 10000 (Sigma-Aldrich); $p16^{INK4}$ (#554079), 1 : 2500 (BD Bioscience, San Jose, CA); ANT3 (AP12188), 1 : 2500 (Abgent, San Diego, CA); HSC70 (SPC-102), 1 : 5000 (StressMarq, Victoria, BC, Canada), HSP72 (ADI-SPA-812-D), 1 : 5000 (Enzo Life Sciences, Farmingdale, NY); HSP60 (MS-120), 1 : 5000 (Thermo Fisher Scientific, Waltham, MA); HMGB1 (PCRP-HMGB1–6E1), 1 : 1000 (Developmental Studies Hybridoma Bank, Iowa City, IA). Chemiluminescence signals of immunoblots were visualized by SuperSignal West Pico and Femto chemiluminescence kits (Thermo Fisher Scientific), captured by ChemiDoc XRS+ (Bio-Rad, , Hercules, CA), and analyzed by Image Lab software (Bio-Rad) for densitometry.

Cell viability, cycle, and death analyses

Cell viability was determined by trypan blue exclusion assay (Invitrogen) or by flow cytometry of cells stained with the fluorescent DNA intercalator TO-PRO 3 (Invitrogen). The colorimetric 3-(4,5-dimethyl-2-thiazolyl)-2,5-diphenyltetrazolium bromide (MTT, Sigma-Aldrich) assay was performed as previously described[19]. For cell cycle and death analyses, flow cytometry of cells stained with annexin V and propidium iodide (Invitrogen) was performed using the Guava EasyCyte flowcytometry system (MilliporeSigma, Billerica, MA, USA), as previously described[47]. Data were analyzed by FCS EXPRESS software (De Novo Software, Los Angeles, CA, USA).

Calcein retention assay

Mitochondrial membrane permeability was analyzed using MitoProbe Transition Pore Assay kit (Thermo Fisher Scientific), according to the manufacturer's instruction. Calcein fluorescence retaining in cells after cobalt quenching was determined by the Guava EasyCyte flowcytometry system (MilliporeSigma) and FCS EXPRESS software (De Novo Software).

Immunohistochemistry

Formalin-fixed, paraffin-embedded 5 μm sections of non-overlapping PDAC tissue microarrays (PA207), containing 51 PDAC cases and 17 normal pancreatic duct samples, were purchased from US Biomax (Rockville, MD). All tissue samples consisted of uniform cores, 1 mm in diameter. The specimens were analyzed using monoclonal anti-mortalin antibody, D-9 (Santa Cruz Biotechnology, sc-133137), as previously described[59]. The specificity of this staining was validated with normal IgG type 2.

Xenograft experiments

Two million cells in 200 μL Hank's balanced salt solution were subcutaneously inoculated into the rear flanks of 5-week-old female athymic nude (nu/nu) mice (The Jackson laboratory, Bar Harbour, ME, USA). Once palpable, tumors were measured using Vernier calipers every other day. Tumor volumes were calculated using the formula: length×width×height×0.5236. When tumor volumes reached about 50 mm^3, mice bearing

each cell line were sorted into three groups to achieve equal distribution of tumor size in all the treatment groups. Group 1 intraperitoneally received 12 doses of the vehicle (1:1.8:0.4:6.8 mixture of DMSO, Kolliphor RH40, dextrose, and HEPES) while groups 2 and 3 received 12 doses of JG-231 (2 and 4 mg/kg body weight/dose, respectively). At the end of the experiment, animals were euthanized by CO_2 asphyxiation. Investigators were not blinded. All animal studies were performed according to the protocols approved by the Institutional Animal Care and Use Committee at Medical College of Wisconsin, Milwaukee, WI, USA.

Quantification and statistical analysis

All graphs represent the mean ± the standard error of the mean (SEM) of technical replicates (*n*) in a representative experiments. All experiments, excluding immunohistochemistry and animal work, were repeated at least three times to confirm data consistency. Sample size of the animal experiment was determined by the power analysis that considered 10% of accidental death and a significance level 5% and was based upon in vitro data. Statistical significance was determined by one-way ANOVA with Dunnett post-tests or two-way ANOVA with Bonferroni post-tests using Prism (GraphPad Software, La Jolla, CA, USA). IC_{50}, Confidence Intervals, coefficient of variation (%CV) and data normality (normal distribution) were determined by Prism. The significance of immunohistochemistry data of human PDAC tissues was determined by Kruskal-Wallis test (nonparametric ANOVA).

Supplementary Material

Refer to Web version on PubMed Central for supplementary material.

Acknowledgement

We thank Drs. Yuri Lazebnik (CSHL), Richard Mulligan (Harvard Univ.), Bert Vogelstein (Johns Hopkins Univ.), and Bob Deschenes (Univ. South Florida) for IMR90E1A, pHAGE, HCT116 cell lines, and the K-Ras^{G12V}– encoding gene, respectively. We also thank former Park lab members for technical supports.

Funding

This work was supported by NIH/National Cancer Institute grant (R01CA138441) to J.P. Development of HSP70 modulators was funded by NIH R01NS059690 to J.G.

Abbreviations:

ANT	adenine nucleotide translocase
c-lamin A	cleaved lamin A
CypD	cyclophilin D
ERK	extracellular signal-regulated kinase
HA	hemagglutinin
HSP	heat shock protein
IC_{50}	half maximal inhibitory concentration

MCU	mitochondrial Ca^{2+} uniporter
MEK	mitogen-activated protein kinase kinase
MPTP	mitochondrial permeability transition pore
PARP	Poly (ADP-ribose) polymerase
PDAC	pancreatic ductal adenocarcinoma

REFERENCES AND NOTE

1. Bailey JM, Hendley AM, Lafaro KJ, Pruski MA, Jones NC, Alsina J et al. p53 mutations cooperate with oncogenic Kras to promote adenocarcinoma from pancreatic ductal cells. Oncogene 2016; 35: 4282–4288. [PubMed: 26592447]
2. Bonora M, Wieckowski MR, Chinopoulos C, Kepp O, Kroemer G, Galluzzi L et al. Molecular mechanisms of cell death: central implication of ATP synthase in mitochondrial permeability transition. Oncogene 2015; 34: 1475–1486. [PubMed: 24727893]
3. Bonora M, Pinton P. A New Current for the Mitochondrial Permeability Transition. Trends Biochem Sci 2019; 44: 559–561. [PubMed: 31076251]
4. Broekemeier KM, Krebsbach RJ, Pfeiffer DR. Inhibition of the mitochondrial Ca2+ uniporter by pure and impure ruthenium red. Mol Cell Biochem 1994; 139: 33–40. [PubMed: 7531818]
5. Bryant KL, Mancias JD, Kimmelman AC, Der CJ. KRAS: feeding pancreatic cancer proliferation. Trends Biochem Sci 2014; 39: 91–100. [PubMed: 24388967]
6. Canon J, Rex K, Saiki AY, Mohr C, Cooke K, Bagal D et al. The clinical KRAS(G12C) inhibitor AMG 510 drives anti-tumour immunity. Nature 2019; 575: 217–223. [PubMed: 31666701]
7. Chen KH, Dasgupta A, Ding J, Indig FE, Ghosh P, Longo DL. Role of mitofusin 2 (Mfn2) in controlling cellular proliferation. FASEB J 2014; 28: 382–394. [PubMed: 24081906]
8. Chevrollier A, Loiseau D, Reynier P, Stepien G. Adenine nucleotide translocase 2 is a key mitochondrial protein in cancer metabolism. Biochim Biophys Acta 2011; 1807: 562–567. [PubMed: 20950584]
9. Crompton M, Barksby E, Johnson N, Capano M. Mitochondrial intermembrane junctional complexes and their involvement in cell death. Biochimie 2002; 84: 143–152. [PubMed: 12022945]
10. Cui X, Li Z, Piao J, Li J, Li L, Lin Z et al. Mortalin expression in pancreatic cancer and its clinical and prognostic significance. Hum Pathol 2017; 64: 171–178. [PubMed: 28412209]
11. Daugaard M, Rohde M, Jaattela M. The heat shock protein 70 family: Highly homologous proteins with overlapping and distinct functions. FEBS Lett 2007; 581: 3702–3710. [PubMed: 17544402]
12. Green DR, Galluzzi L, Kroemer G. Cell biology. Metabolic control of cell death. Science 2014; 345: 1250256. [PubMed: 25237106]
13. Halestrap AP, Connern CP, Griffiths EJ, Kerr PM. Cyclosporin A binding to mitochondrial cyclophilin inhibits the permeability transition pore and protects hearts from ischaemia/reperfusion injury. Mol Cell Biochem 1997; 174: 167–172. [PubMed: 9309682]
14. Halestrap AP, Woodfield KY, Connern CP. Oxidative stress, thiol reagents, and membrane potential modulate the mitochondrial permeability transition by affecting nucleotide binding to the adenine nucleotide translocase. J Biol Chem 1997; 272: 3346–3354. [PubMed: 9013575]
15. Halestrap AP, Brenner C. The adenine nucleotide translocase: a central component of the mitochondrial permeability transition pore and key player in cell death. Curr Med Chem 2003; 10: 1507–1525. [PubMed: 12871123]
16. Haq R, Shoag J, Andreu-Perez P, Yokoyama S, Edelman H, Rowe GC et al. Oncogenic BRAF regulates oxidative metabolism via PGC1alpha and MITF. Cancer Cell 2013; 23: 302–315. [PubMed: 23477830]
17. He J, Ford HC, Carroll J, Ding S, Fearnley IM, Walker JE. Persistence of the mitochondrial permeability transition in the absence of subunit c of human ATP synthase. Proc Natl Acad Sci U S A 2017; 114: 3409–3414. [PubMed: 28289229]

18. Hong SK, Yoon S, Moelling C, Arthan D, Park JI. Noncatalytic function of ERK1/2 can promote Raf/MEK/ERK-mediated growth arrest signaling. J Biol Chem 2009; 284: 33006–33018. [PubMed: 19805545]
19. Hong SK, Wu PK, Park JI. A cellular threshold for active ERK1/2 levels determines Raf/MEK/ERK-mediated growth arrest versus death responses. Cell Signal 2018; 42: 11–20. [PubMed: 28986121]
20. Hoshino A, Wang WJ, Wada S, McDermott-Roe C, Evans CS, Gosis B et al. The ADP/ATP translocase drives mitophagy independent of nucleotide exchange. Nature 2019; 575: 375–379. [PubMed: 31618756]
21. Humpton TJ, Alagesan B, DeNicola GM, Lu D, Yordanov GN, Leonhardt CS et al. Oncogenic KRAS Induces NIX-Mediated Mitophagy to Promote Pancreatic Cancer. Cancer Discov 2019; 9: 1268–1287. [PubMed: 31263025]
22. Hurst S, Baggett A, Csordas G, Sheu SS. SPG7 targets the m-AAA protease complex to process MCU for uniporter assembly, Ca(2+) influx, and regulation of mitochondrial permeability transition pore opening. J Biol Chem 2019; 294: 10807–10818. [PubMed: 31097542]
23. Karkhanis M, Park JI. Sp1 regulates Raf/MEK/ERK-induced p21 transcription in TP53-mutated cancer cells. Cell Signal 2015; 27: 479–486. [PubMed: 25595558]
24. Karoulia Z, Gavathiotis E, Poulikakos PI. New perspectives for targeting RAF kinase in human cancer. Nat Rev Cancer 2017; 17: 676–691. [PubMed: 28984291]
25. Kaul SC, Deocaris CC, Wadhwa R. Three faces of mortalin: a housekeeper, guardian and killer. Exp Gerontol 2007; 42: 263–274. [PubMed: 17188442]
26. Khalil AA, Kabapy NF, Deraz SF, Smith C. Heat shock proteins in oncology: Diagnostic biomarkers or therapeutic targets? Biochim Biophys Acta 2011; 1816: 89–104. [PubMed: 21605630]
27. Kidger AM, Sipthorp J, Cook SJ. ERK1/2 inhibitors: New weapons to inhibit the RAS-regulated RAF-MEK1/2-ERK1/2 pathway. Pharmacol Ther 2018; 187: 45–60. [PubMed: 29454854]
28. Konieczkowski DJ, Johannessen CM, Garraway LA. A Convergence-Based Framework for Cancer Drug Resistance. Cancer Cell 2018; 33: 801–815. [PubMed: 29763622]
29. Koya K, Li Y, Wang H, Ukai T, Tatsuta N, Kawakami M et al. MKT-077, a novel rhodacyanine dye in clinical trials, exhibits anticarcinoma activity in preclinical studies based on selective mitochondrial accumulation. Cancer Res 1996; 56: 538–543. [PubMed: 8564968]
30. Kroemer G, Galluzzi L, Brenner C. Mitochondrial membrane permeabilization in cell death. Physiol Rev 2007; 87: 99–163. [PubMed: 17237344]
31. Leanza L, Zoratti M, Gulbins E, Szabo I. Mitochondrial ion channels as oncological targets. Oncogene 2014; 33: 5569–5581. [PubMed: 24469031]
32. Lee AS. Glucose-regulated proteins in cancer: molecular mechanisms and therapeutic potential. Nat Rev Cancer 2014; 14: 263–276. [PubMed: 24658275]
33. Lu WJ, Lee NP, Kaul SC, Lan F, Poon RT, Wadhwa R et al. Mortalin-p53 interaction in cancer cells is stress dependent and constitutes a selective target for cancer therapy. Cell death and differentiation 2011; 18: 1046–1056. [PubMed: 21233847]
34. Maruta H, Tikoo A, Shakri R, Shishido T. The anti-RAS cancer drug MKT-077 is an F-actin cross-linker. Ann N Y Acad Sci 1999; 886: 283–284. [PubMed: 10667240]
35. Miyata Y, Li X, Lee HF, Jinwal UK, Srinivasan SR, Seguin SP et al. Synthesis and initial evaluation of YM-08, a blood-brain barrier permeable derivative of the heat shock protein 70 (Hsp70) inhibitor MKT-077, which reduces tau levels. ACS Chem Neurosci 2013; 4: 930–939. [PubMed: 23472668]
36. Modica-Napolitano JS, Aprille JR. Delocalized lipophilic cations selectively target the mitochondria of carcinoma cells. Adv Drug Deliv Rev 2001; 49: 63–70. [PubMed: 11377803]
37. Na Y, Kaul SC, Ryu J, Lee JS, Ahn HM, Kaul Z et al. Stress chaperone mortalin contributes to epithelial-mesenchymal transition and cancer metastasis. Cancer Res 2016; 76: 2754–2765. [PubMed: 26960973]
38. Nagdas S, Kashatus JA, Nascimento A, Hussain SS, Trainor RE, Pollock SR et al. Drp1 Promotes KRas-Driven Metabolic Changes to Drive Pancreatic Tumor Growth. Cell Rep 2019; 28: 1845–1859 e1845. [PubMed: 31412251]

39. Neginskaya MA, Solesio ME, Berezhnaya EV, Amodeo GF, Mnatsakanyan N, Jonas EA et al. ATP Synthase C-Subunit-Deficient Mitochondria Have a Small Cyclosporine A-Sensitive Channel, but Lack the Permeability Transition Pore. Cell Rep 2019; 26: 11–17 e12. [PubMed: 30605668]
40. Ostrem JM, Peters U, Sos ML, Wells JA, Shokat KM. K-Ras(G12C) inhibitors allosterically control GTP affinity and effector interactions. Nature 2013; 503: 548–551. [PubMed: 24256730]
41. Rosen A, Casciola-Rosen L. Macromolecular substrates for the ICE-like proteases during apoptosis. J Cell Biochem 1997; 64: 50–54. [PubMed: 9015754]
42. Rousaki A, Miyata Y, Jinwal UK, Dickey CA, Gestwicki JE, Zuiderweg ER. Allosteric drugs: the interaction of antitumor compound MKT-077 with human Hsp70 chaperones. J Mol Biol 2011; 411: 614–632. [PubMed: 21708173]
43. Rozenberg P, Kocsis J, Saar M, Prohaszka Z, Fust G, Fishelson Z. Elevated levels of mitochondrial mortalin and cytosolic HSP70 in blood as risk factors in patients with colorectal cancer. Int J Cancer 2013; 133: 514–518. [PubMed: 23319326]
44. Sale MJ, Cook SJ. Intrinsic and acquired resistance to MEK1/2 inhibitors in cancer. Biochem Soc Trans 2014; 42: 776–783. [PubMed: 25109957]
45. Santo-Domingo J, Vay L, Hernandez-Sanmiguel E, Lobaton CD, Moreno A, Montero M et al. The plasma membrane Na+/Ca2+ exchange inhibitor KB-R7943 is also a potent inhibitor of the mitochondrial Ca2+ uniporter. Br J Pharmacol 2007; 151: 647–654. [PubMed: 17471180]
46. Shao H, Li X, Moses MA, Gilbert LA, Kalyanaraman C, Young ZT et al. Exploration of Benzothiazole Rhodacyanines as Allosteric Inhibitors of Protein-Protein Interactions with Heat Shock Protein 70 (Hsp70). J Med Chem 2018; 61: 6163–6177. [PubMed: 29953808]
47. Starenki D, Park JI. Mitochondria-targeted nitroxide, Mito-CP, suppresses medullary thyroid carcinoma cell survival in vitro and in vivo. J Clin Endocrinol Metab 2013; 98: 1529–1540. [PubMed: 23509102]
48. Starenki D, Hong SK, Lloyd RV, Park JI. Mortalin (GRP75/HSPA9) upregulation promotes survival and proliferation of medullary thyroid carcinoma cells. Oncogene 2015; 34: 4624–4634. [PubMed: 25435367]
49. Sun J, Che SL, Piao JJ, Xu M, Chen LY, Lin ZH. Mortalin overexpression predicts poor prognosis in early stage of non-small cell lung cancer. Tumour Biol 2017; 39: 1010428317695918.
50. Utkina-Sosunova IV, Niatsetskaya ZV, Sosunov SA, Ratner VI, Matsiukevich D, Ten VS. Nelfinavir inhibits intra-mitochondrial calcium influx and protects brain against hypoxic-ischemic injury in neonatal mice. PLoS One 2013; 8: e62448. [PubMed: 23614049]
51. Vasan N, Baselga J, Hyman DM. A view on drug resistance in cancer. Nature 2019; 575: 299–309. [PubMed: 31723286]
52. Vaseva AV, Marchenko ND, Ji K, Tsirka SE, Holzmann S, Moll UM. p53 opens the mitochondrial permeability transition pore to trigger necrosis. Cell 2012; 149: 1536–1548. [PubMed: 22726440]
53. Viale A, Pettazzoni P, Lyssiotis CA, Ying H, Sanchez N, Marchesini M et al. Oncogene ablation-resistant pancreatic cancer cells depend on mitochondrial function. Nature 2014; 514: 628–632. [PubMed: 25119024]
54. Wadhwa R, Takano S, Robert M, Yoshida A, Nomura H, Reddel RR et al. Inactivation of tumor suppressor p53 by mot-2, a hsp70 family member. J Biol Chem 1998; 273: 29586–29591. [PubMed: 9792667]
55. Wadhwa R, Sugihara T, Yoshida A, Nomura H, Reddel RR, Simpson R et al. Selective toxicity of MKT-077 to cancer cells is mediated by its binding to the hsp70 family protein mot-2 and reactivation of p53 function. Cancer Res 2000; 60: 6818–6821. [PubMed: 11156371]
56. Wadhwa R, Takano S, Kaur K, Aida S, Yaguchi T, Kaul Z et al. Identification and characterization of molecular interactions between mortalin/mtHsp70 and HSP60. The Biochemical journal 2005; 391: 185–190. [PubMed: 15957980]
57. Wadhwa R, Takano S, Kaur K, Deocaris CC, Pereira-Smith OM, Reddel RR et al. Upregulation of mortalin/mthsp70/Grp75 contributes to human carcinogenesis. Int J Cancer 2006; 118: 2973–2980. [PubMed: 16425258]
58. Weaver JG, Tarze A, Moffat TC, Lebras M, Deniaud A, Brenner C et al. Inhibition of adenine nucleotide translocator pore function and protection against apoptosis in vivo by an HIV protease inhibitor. J Clin Invest 2005; 115: 1828–1838. [PubMed: 15937550]

59. Wu PK, Hong SK, Veeranki S, Karkhanis M, Starenki D, Plaza JA et al. A Mortalin/HSPA9-Mediated Switch in Tumor-Suppressive Signaling of Raf/MEK/Extracellular Signal-Regulated Kinase. Mol Cell Biol 2013; 33: 4051–4067. [PubMed: 23959801]

60. Wu PK, Hong SK, Park JI. Steady-State Levels of Phosphorylated Mitogen-Activated Protein Kinase Kinase 1/2 Determined by Mortalin/HSPA9 and Protein Phosphatase 1 Alpha in KRAS and BRAF Tumor Cells. Mol Cell Biol 2017; 37: e00061–00017. [PubMed: 28674184]

61. Wu PK, Hong SK, Chen W, Becker AE, Gundry RL, Lin CW et al. Mortalin (HSPA9) facilitates BRAF-mutant tumor cell survival by suppressing ANT3-mediated mitochondrial membrane permeability. Sci Signal 2020; 13: pii: eaay1478. [PubMed: 32156782]

62. Xu M, Jin T, Chen L, Zhang X, Zhu G, Wang Q et al. Mortalin is a distinct bio-marker and prognostic factor in serous ovarian carcinoma. Gene 2019; 696: 63–71. [PubMed: 30776464]

63. Yu M, Nguyen ND, Huang Y, Lin D, Fujimoto TN, Molkentine JM et al. Mitochondrial fusion exploits a therapeutic vulnerability of pancreatic cancer. JCI Insight 2019; 5.

64. Yun CO, Bhargava P, Na Y, Lee JS, Ryu J, Kaul SC et al. Relevance of mortalin to cancer cell stemness and cancer therapy. Sci Rep 2017; 7: 42016. [PubMed: 28165047]

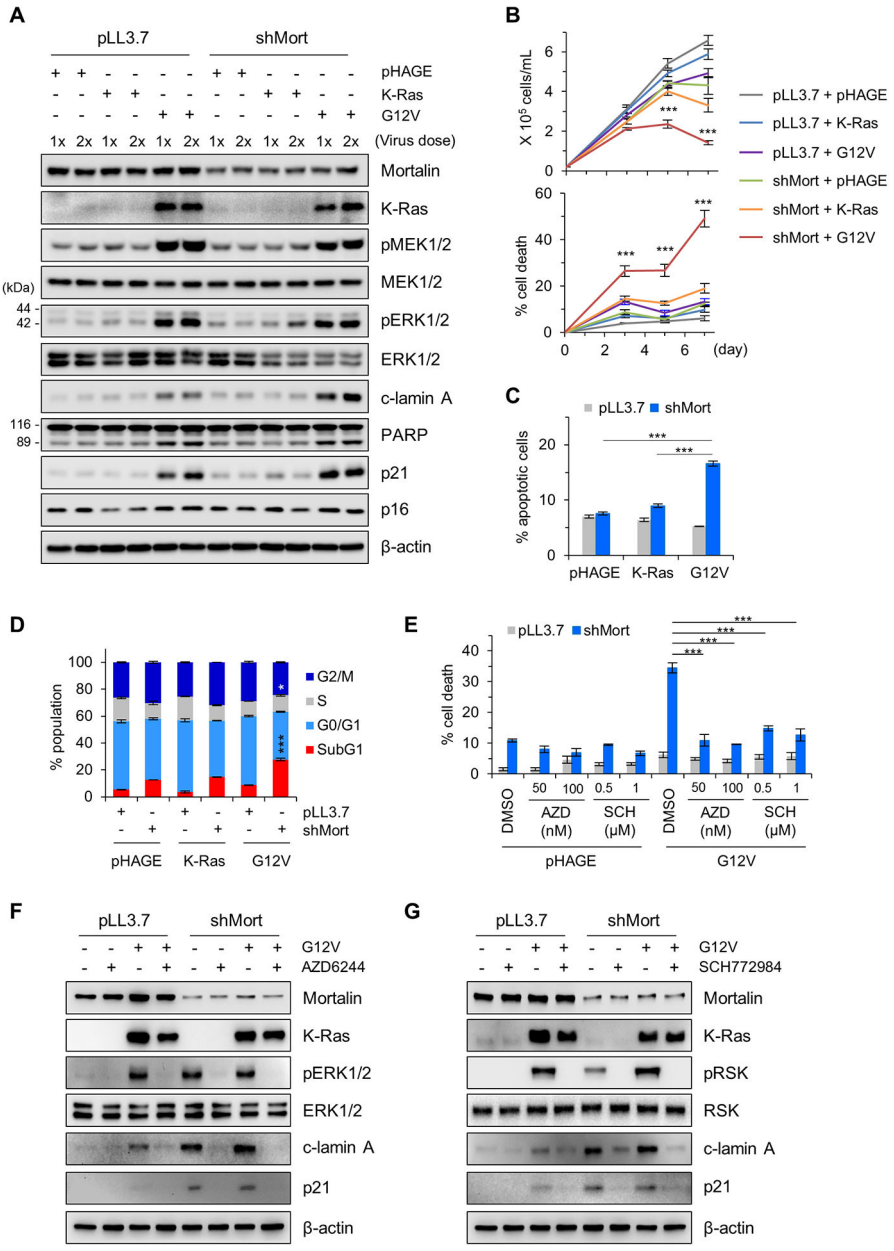

Figure 1. Mortalin depletion selectively suppresses K-Raf^{G12V}-expressing IMR90E1A cells.

(A) Western blotting of total lysates of IMR90E1A cells co-infected with pLL3.7 virus expressing shRNA targeting mortalin (shMort) and pHAGE expressing wild type K-Ras or K-Ras^{G12V} (G12V) for 3 days. pMEK1/2, phosphorylated MEK1/2; pERK1/2, phosphorylated ERK1/2; c-lamin A, cleaved lamin A. β-actin was the control for equal protein loading. **(B)** Proliferation and death rates of cells described in (A), monitored by trypan blue exclusion assays (n = 3). **(C)** Apoptosis rates of cells described in (A) at post-infection day 2, monitored by annexin V/propidium iodide staining and flow cytometry (n = 5). See Figure S1A for FACS histograms. **(D)** Cell cycle analysis of cells described in (A) at post-infection day 3 (n = 3). See Figure S1B for FACS histograms. **(E)** TO-PRO-3 assays of cells co-infected with pLL3.7-shMort and pHAGE-K-Ras^{G12V}, and then treated with

indicated inhibitors for 2 days ($n = 5$). **(F and G)** Western blotting of total lysates of cells described in (E). All quantitative data are mean ± SEM from a representative experiment. *$p < 0.05$, **$p < 0.01$, ***$p < 0.001$ (two-way ANOVA with Bonferroni post-tests)

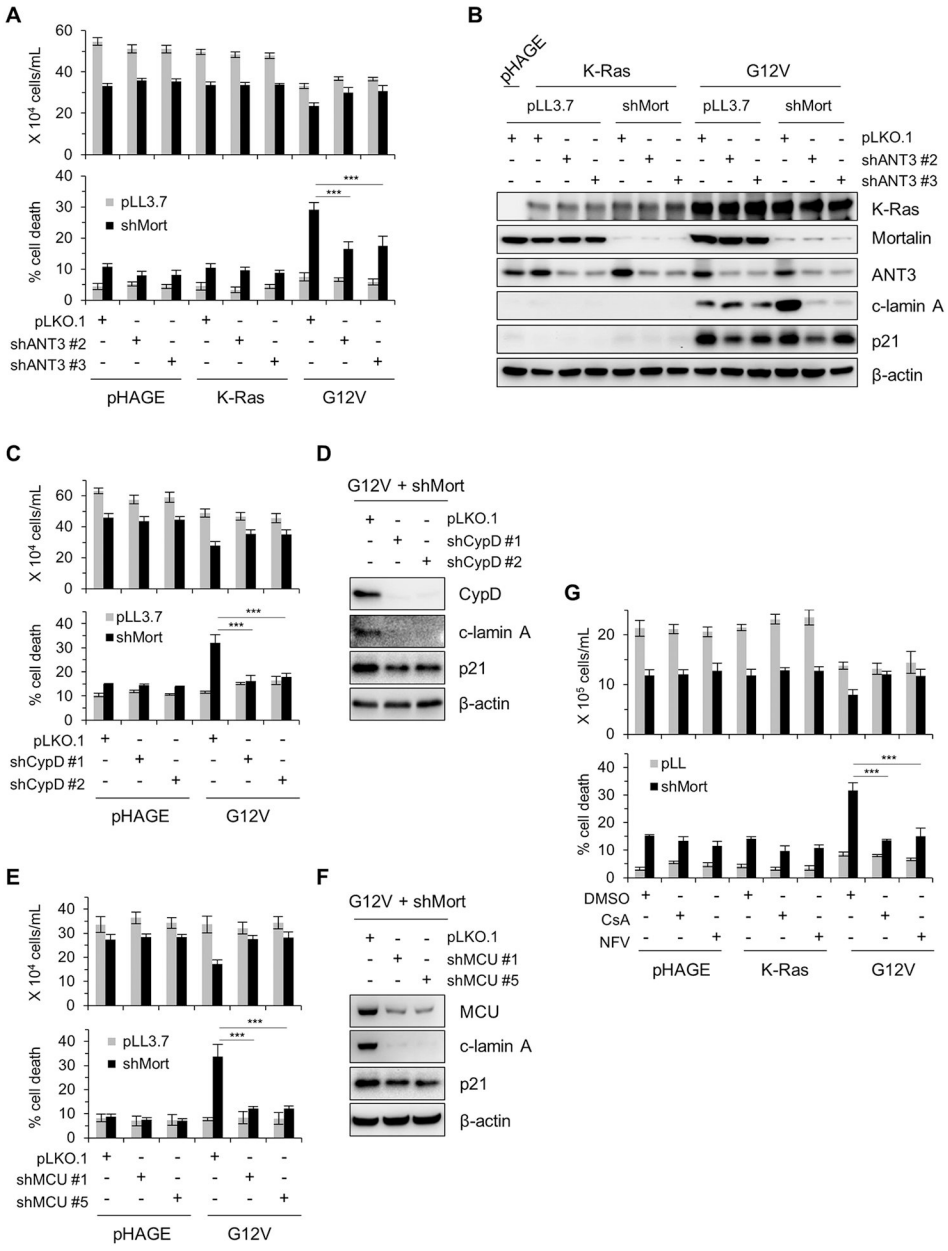

Figure 2. ANT, CypD and MCU are required for mortalin depletion to induce lethality in K-Ras^{G12V}-expressing IMR90E1A cells.

(A) Proliferation and death rates of IMR90E1A cells expressing K-Ras or K-Ras^{G12V} and infected for 4 days with pLL3.7-shMort and pLKO.1-shANT3 viruses (shANT3#2 and shANT3#3 targeting different ANT3 mRNA regions), monitored by TO-PRO-3 assays (n = 5). **(B)** Western blotting of total lysates of cells treated as described in (A). c-lamin A, cleaved lamin A. **(C)** TO-PRO-3 assays of IMR90E1A cells expressing K-Ras or K-Ras^{G12V} and infected for 4 days with pLL3.7-shMort and pLKO.1-shCypD viruses (shCypD#1 and shCypD#2 targeting different CypD mRNA regions) (n = 5). **(D)** Western blotting of total lysates of K-Ras^{G12V}–expressing cells treated as described in (C). **(E)** TO-PRO-3 assays of IMR90E1A cells expressing K-Ras or K-Ras^{G12V} and infected for 4 days with pLL3.7-

shMort and pLKO.1-shMCU viruses (shMCU#1 and shMCU#5 targeting different MCU mRNA regions) ($n = 5$). **(F)** Western blotting of total lysates of K-Ras^{G12V}–expressing cells treated as described in (E). **(G)** TO-PRO-3 assays of IMR90E1A cells expressing K-Ras or K-Ras^{G12V} and depleted of mortalin for 4 days with or without 3-day treatment of 5 μM cyclosporine A (CsA) or 5 μM Nelfinavir (NFV) ($n = 5$). DMSO, vehicle control. All quantitative data are mean ± SEM from a representative experiment. ***$p < 0.001$ (two-way ANOVA with Bonferroni post-tests).

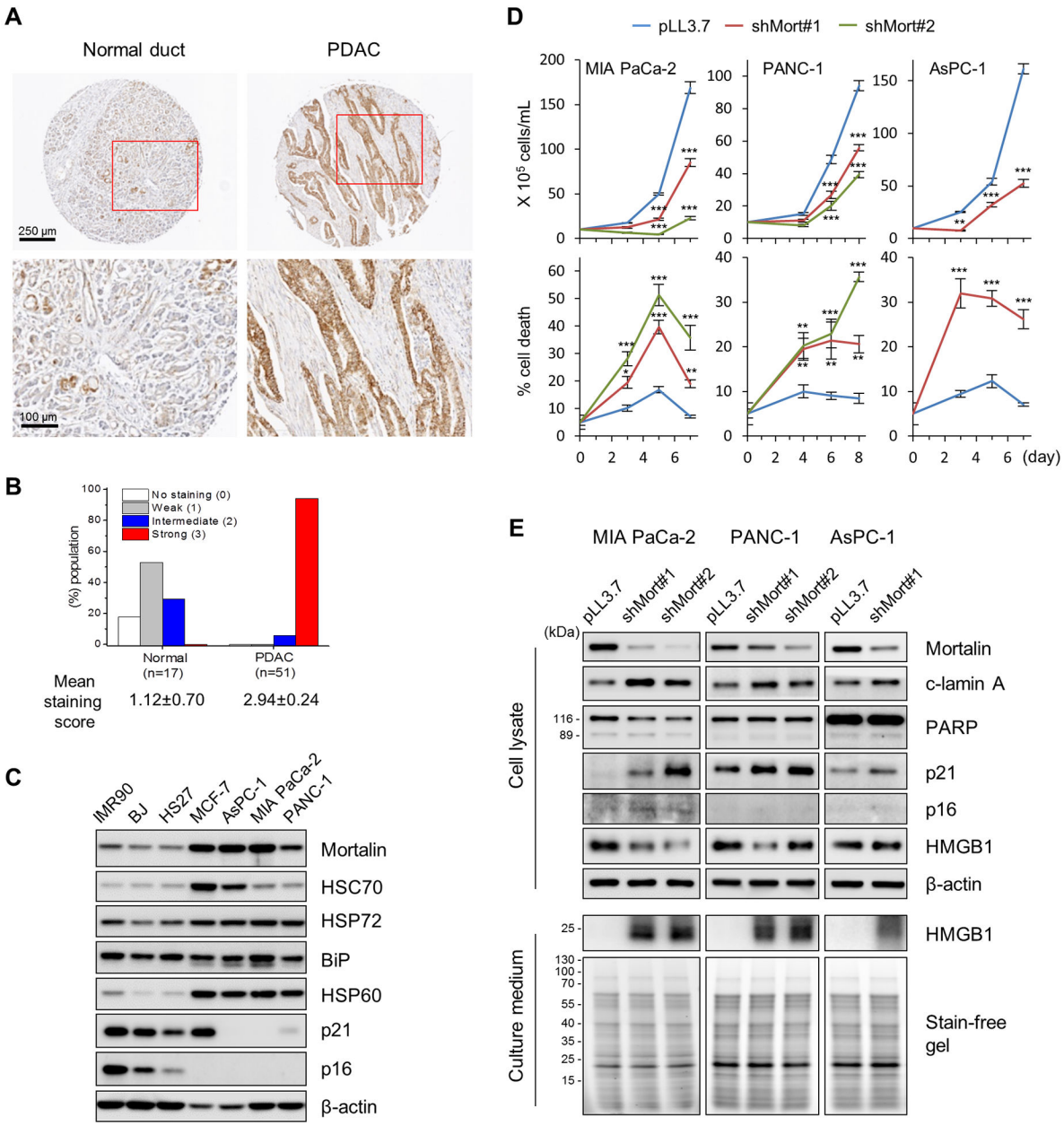

Figure 3. Mortalin is upregulated in PDAC and its depletion suppresses PDAC cells in vitro.

(A) Representative immunohistochemical analysis images of mortalin protein in normal pancreatic duct ($n = 17$) and PDAC ($n = 51$). **(B)** Scores of mortalin expression in patient tissue biopsy specimens. $p < 0.0001$, Kruskal-Wallis test (nonparametric ANOVA). **(C)** Western blotting of total cell lysates of the human PDAC cell lines. The primary normal fibroblasts and MCF-7 breast cancer line were used as the negative and positive controls for mortalin expression, respectively. β-actin was the control for equal protein loading. **(D)** Proliferation and death rates of PDAC cell lines infected with pLL3.7-shMort (shMort#1 and shMort#2 targeting different mortalin mRNA regions), monitored by trypan blue exclusion assays ($n = 3$). Data are mean ± SEM from a representative experiment. *$p < 0.05$, **$p < 0.01$, ***$p < 0.001$ (two-way ANOVA with Bonferroni post-tests) **(E)** Western blotting of

total lysates or culture medium of cells harvested at day 5 (PANC-1) or day 6 (MIA PaCa-2 and AsPC-1) in (D). c-lamin A, cleaved lamin A. Stain-free gel image indicates equal protein loading for HMGB1.

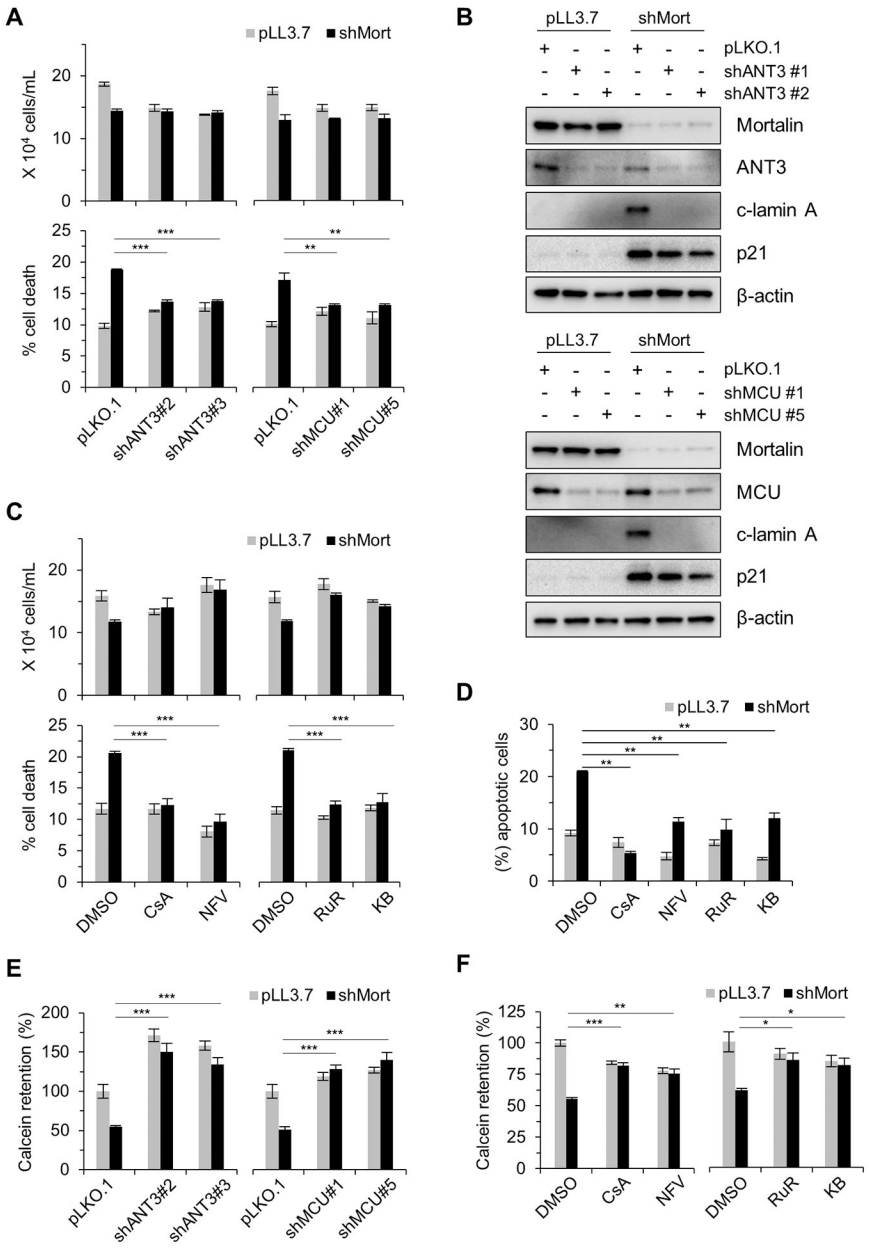

Figure 4. Increased mitochondrial permeability is associated with mitochondrial cell death induced by mortalin depletion in MIA PaCa-2 cells.

(A) Proliferation and death rates of MIA PaCa-2 cells depleted of mortalin with or without 4-day infection with pLKO.1-shANT3 or pLKO.1-shMCU viruses, monitored by TO-PRO-3 assays ($n = 5$). **(B)** Western blotting of total lysate of cells treated as described in (A). c-lamin A, cleaved lamin A. **(C)** TO-PRO-3 assays of MIA PaCa-2 cells depleted of mortalin with or without 3-day treatment of 5 μM cyclosporine A (CsA), 5 μM Nelfinavir (NFV), 4 μM ruthenium red (RuR), or 4 μM KB-R7943 (KB) ($n = 5$). DMSO, vehicle control. **(D)** Apoptosis rates of cells treated as described in (C), monitored by annexin V/propidium iodide staining and flow cytometry ($n = 5$). See Figure S2 for FACS histograms. **(E-F)** Calcein retention assays of cells described in (A and C) ($n = 5$). See Figures S3, A and B for

FACS histograms. Data are mean ± SEM from a representative experiment. *$p < 0.05$, **$p < 0.01$, ***$p < 0.001$ (two-way ANOVA with Bonferroni post-tests)

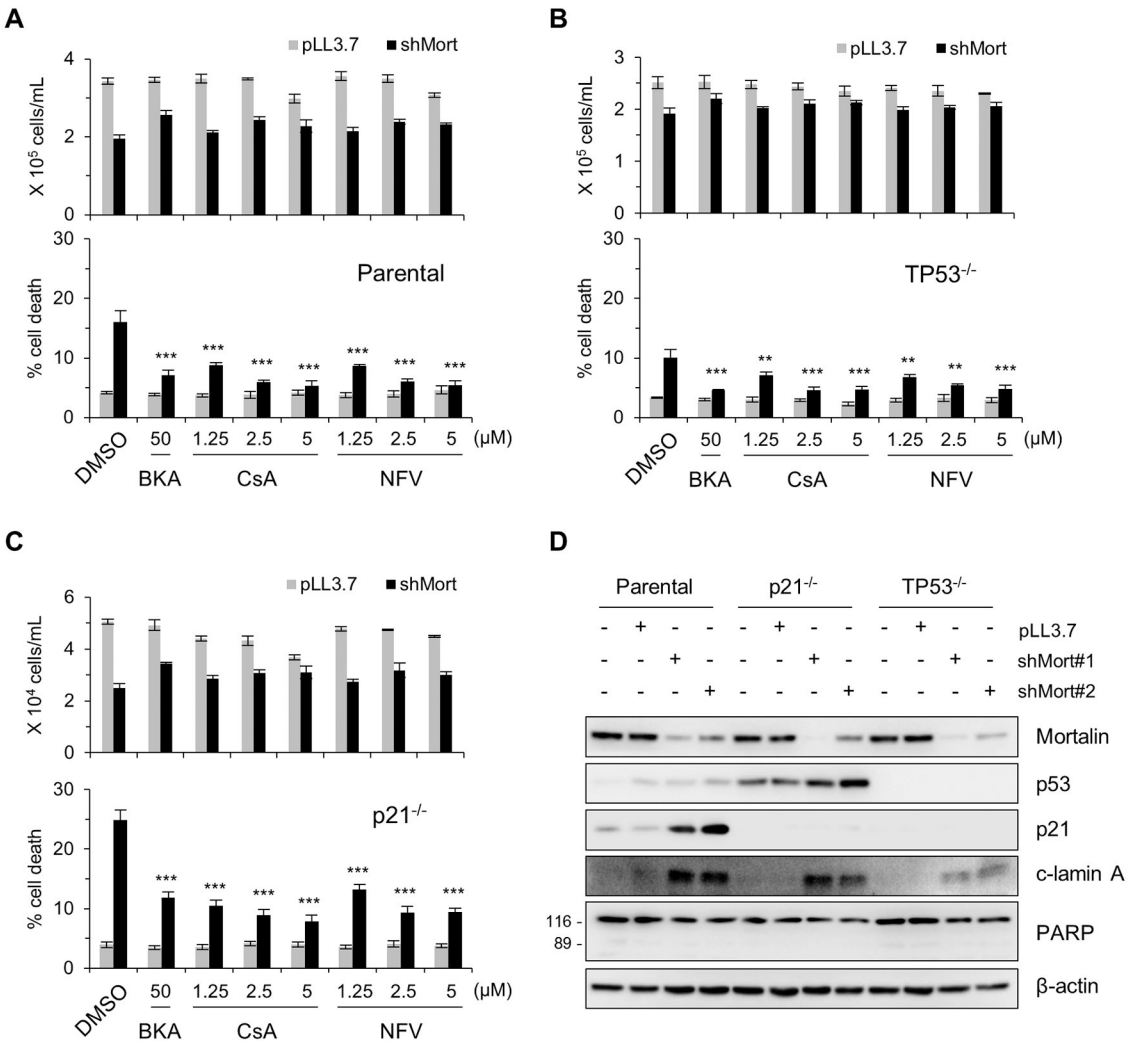

Figure 5. TP53 and p21 are not necessary for mortalin depletion to induce mitochondrial cell death.

(A) Proliferation and death rates of HCT116 parental cells depleted of mortalin with or without 3-day treatment of bongkrekic acid (BKA), cyclosporine A (CsA), Nelfinavir (NFV) at indicated concentration, monitored by TO-PRO-3 assays ($n = 5$). **(B)** Proliferation and death rates of HCT116 TP53 knockout ($TP53^{-/-}$) cells treated as described in (A) ($n = 5$). **(C)** Proliferation and death rates of HCT116 p21 knockout ($p21^{-/-}$) cells treated as described in (A) ($n = 5$). **(D)** Western blotting of total lysate of cells treated as described in (A-C). c-lamin A, cleaved lamin A. Data are mean ± SEM from a representative experiment. $^{*}p < 0.05$, $^{**}p < 0.01$, $^{***}p < 0.001$ (two-way ANOVA with Bonferroni post-tests).

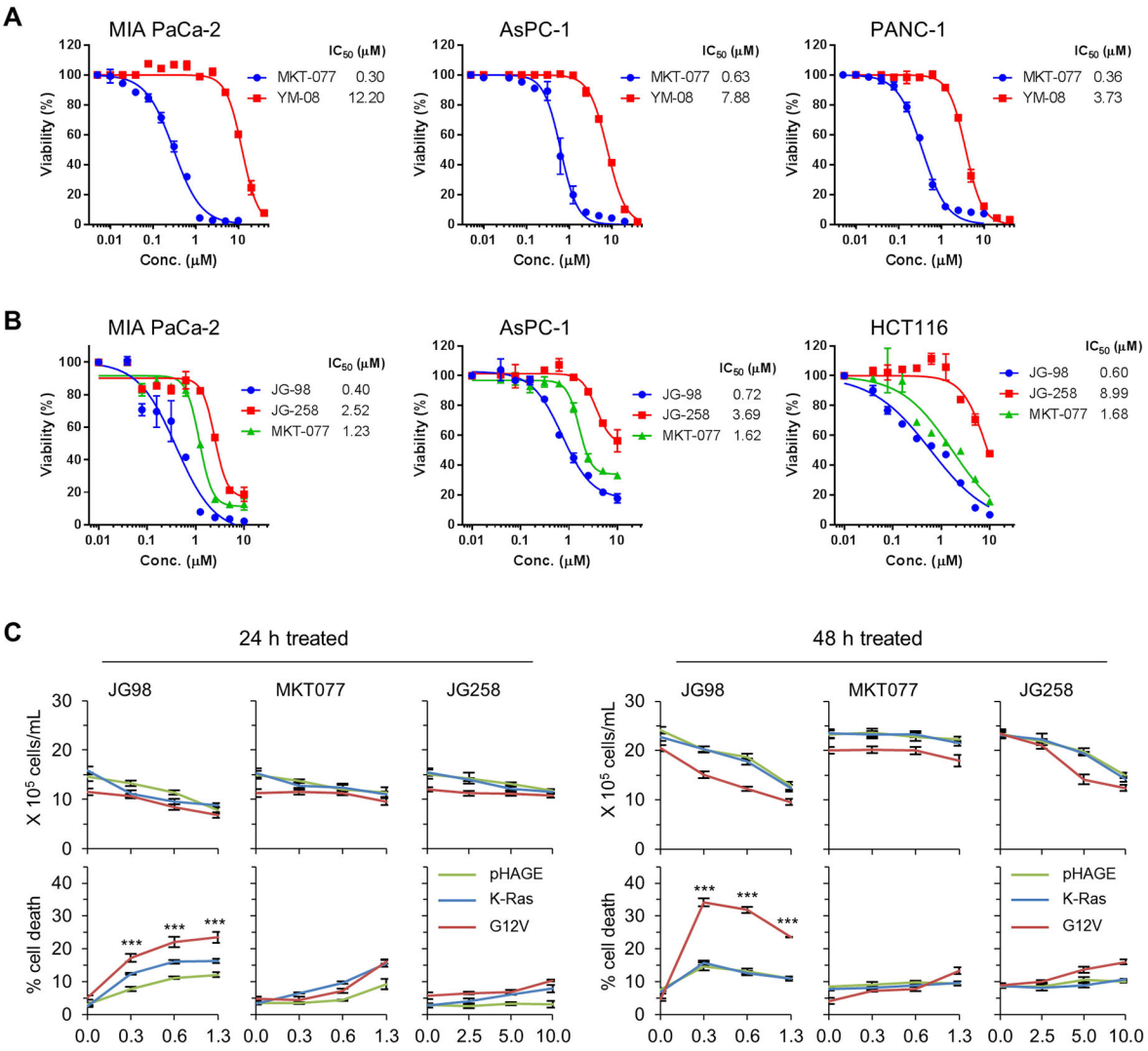

Figure 6. MKT-077 derivatives suppress K-Ras^{mut}-expressing IMR90E1A and tumor cells

(A) IC_{50} analysis in *KRAS* mutant tumor cells treated with MKT-077 and YM-08, a $\Delta\psi_m$-insensitive neutral derivative of MKT-077, for 48 hours, determined by MTT assay ($n = 5$). 95% Confidence Intervals for MKT-077 vs YM-08 were 0.27 to 0.34 vs 11.21 to13.29 (MIA PaCa-2), 0.55 to 0.73 vs 7.55 to 8.22 (AsPC-1), and 0.33 to 0.40 vs 3.53 to 3.93 (PANC-1). **(B)** IC_{50} analysis in *KRAS* mutant tumor cells treated with JG-98, MKT-077, and JG-258, a functional moiety-lacking control for JG-98, for 48 hours, determined by MTT assay ($n = 5$). 95% Confidence Intervals for JG-98 vs MKT-077 were 0.25 to 0.65 vs 1.10 to 1.38 (MIA PaCa-2), 0.60 to 0.86 vs 1.47 to 1.78 (AsPC-1), 0.50 to 0.74 vs 1.27 to 2.23 (HCT116). **(C)** Proliferation and death rates of IMR90E1A cells expressing K-Ras or K-Ras^{G12V} treated with MKT-077 derivatives for 24 and 48 hours prior to trypan blue exclusion assays ($n = 5$). Data are mean ± SEM from a representative experiment. *$p < 0.05$, **$p < 0.01$, ***$p < 0.001$ (two-way ANOVA with Bonferroni post-tests)

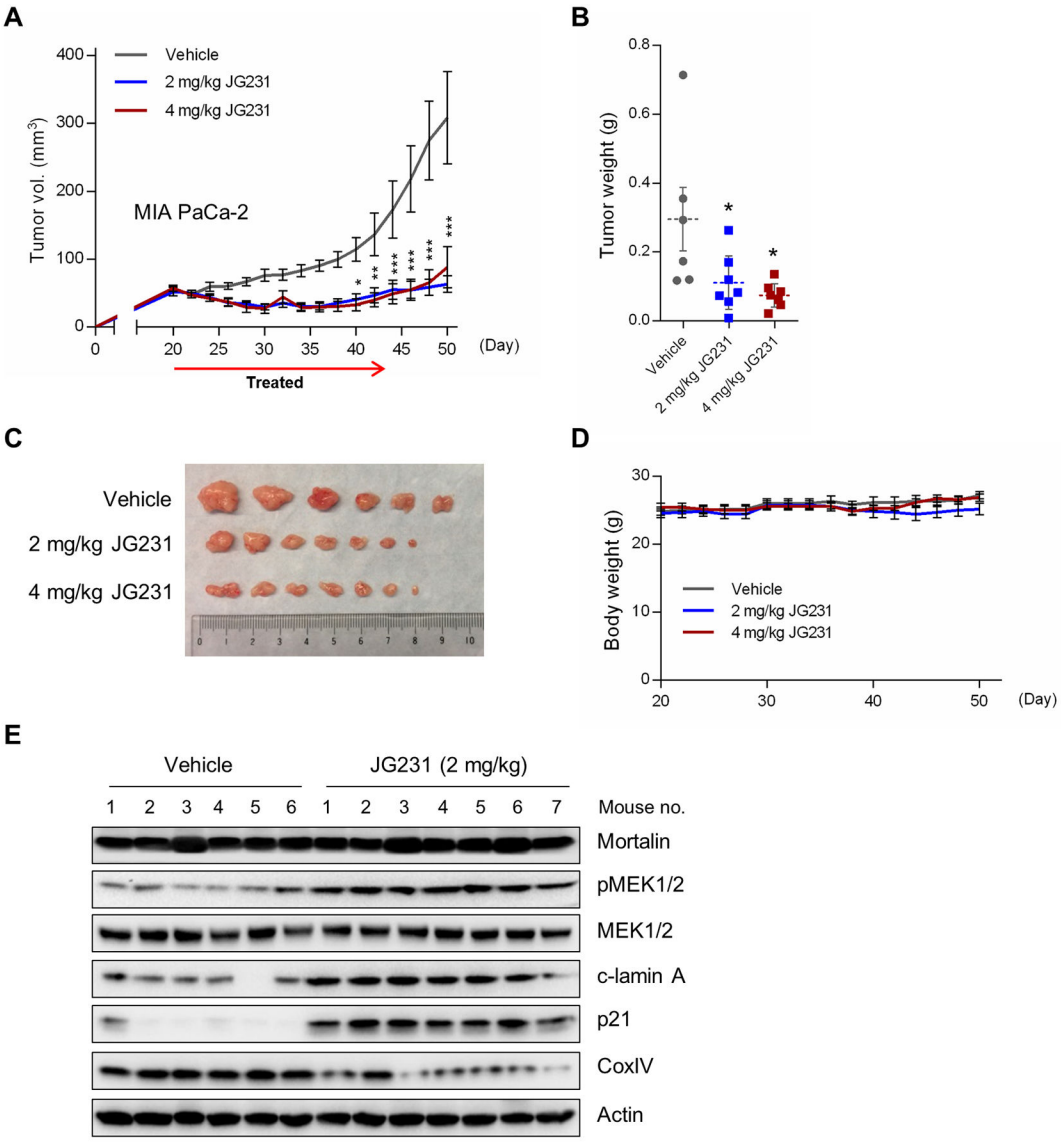

Figure 7. JG-231 suppresses MIA PaCa-2 xenografts in mice

(A) Changes in tumor sizes. Athymic mice bearing tumor xenografts were treated with JG-231 at two different doses. Drugs dissolved in 200 μl vehicle were administered intraperitoneally every other day during indicated treatment periods. The control group was treated with the vehicle only (details in the methods section). %CV, vehicle: 73.11; 2 mg/kg JG-231: 36.67; 4 mg/kg JG-231: 46.27. **(B and C)** Weights and images of tumors collected at the end of the treatment in (A). Horizontal dotted line indicates mean. Each dot represents one sample. %CV, vehicle: 76.67; 2 mg/kg JG-231: 76.22; 4 mg/kg JG-231: 49.35. **(D)** Body weight changes of animals during the treatment in (A). %CV, vehicle: 2.87; 2 mg/kg JG-231: 1.95; 4 mg/kg JG-231: 2.59. **(E)** Western blotting of the homogenates of tumors in (C). c-lamin A, cleaved lamin A; CoxIV, cytochrome *c* oxidase. Data are mean ± SEM from a single cohort (6 mice for vehicle, 7 mice for each JG-231 group). Each mouse developed

one tumor. *$p < 0.05$, **$p < 0.01$, ***$p < 0.001$ (**A** and **D**, two-way ANOVA with Bonferroni post-tests; **B**, one-way ANOVA with Dunnett post-tests)